APPLIED AND ENVIRONMENTAL MICROBIOLOGY, Jan. 2009, p. 493–503 Vol. 75, No. 2
0099-2240/09/$08.00+0 doi:10.1128/AEM.02077-08

Production of Pyomelanin, a Second Type of Melanin, via the Tyrosine Degradation Pathway in *Aspergillus fumigatus*▽

Jeannette Schmaler-Ripcke,[1]† Venelina Sugareva,[1]†‡ Peter Gebhardt,[2] Robert Winkler,[2] Olaf Kniemeyer,[1] Thorsten Heinekamp,[1] and Axel A. Brakhage[1]*

Department of Molecular and Applied Microbiology[1] and Department of Biomolecular Chemistry,[2] Leibniz Institute for Natural Product Research and Infection Biology, Hans Knöll Institute and Friedrich Schiller University Jena, Beutenbergstrasse 11a, 07745 Jena, Germany

Received 8 September 2008/Accepted 14 November 2008

***Aspergillus fumigatus* is the most important airborne fungal pathogen of immunosuppressed humans. *A. fumigatus* is able to produce dihydroxynaphthalene melanin, which is predominantly present in the conidia. Its biosynthesis is an important virulence determinant. Here, we show that *A. fumigatus* is able to produce an alternative melanin, i.e., pyomelanin, by a different pathway, starting from L-tyrosine. Proteome analysis indicated that the L-tyrosine degradation enzymes are synthesized when the fungus is grown with L-tyrosine in the medium. To investigate the pathway in detail, we deleted the genes encoding essential enzymes for pigment production, homogentisate dioxygenase (*hmgA*) and 4-hydroxyphenylpyruvate dioxygenase (*hppD*). Comparative Fourier transform infrared spectroscopy of synthetic pyomelanin and pigment extracted from *A. fumigatus* cultures confirmed the identity of the observed pigment as pyomelanin. In the *hmgA* deletion strain, HmgA activity was abolished and the accumulation of homogentisic acid provoked an increased pigment formation. In contrast, homogentisic acid and pyomelanin were not observed with an *hppD* deletion mutant. Germlings of the *hppD* deletion mutant showed an increased sensitivity to reactive oxygen intermediates. The transcription of both studied genes was induced by L-tyrosine. These results confirmed the function of the deleted genes and the predicted pathway in *A. fumigatus*. Homogentisic acid is the major intermediate, and the L-tyrosine degradation pathway leading to pyomelanin is similar to that in humans leading to alkaptomelanin.**

Aspergillus fumigatus is the most important airborne human-pathogenic fungus. In immunocompromised patients, *A. fumigatus* has the potential to cause a life-threatening disease called invasive aspergillosis (IA). In the last two decades, the incidence of IA has increased tremendously. Specific diagnostics are still limited, as are therapeutic interventions. As a result, the mortality of IA is very high, ranging between 50 and 90% despite therapy (for an overview, see references 4, 38, 41, and 50).

A. fumigatus possesses specific physiological and molecular characteristics which make this fungus an aggressive pathogen (2, 41). These include the biosynthesis of a certain type of melanin, i.e., dihydroxynaphthalene (DHN) melanin, which is present in the gray-green conidia. Green fluorescent protein fusion with the polyketide synthase gene *pksP*, which is involved in DHN melanin biosynthesis, proved that this gene is transcribed in hyphae of germinating conidia isolated from lungs of infected immunosuppressed mice (31). PksP is also involved in the inhibition of phagosome-lysosome fusion and, thereby, the killing of *A. fumigatus* conidia (23). Additionally, DHN melanin has been shown to protect *A. fumigatus* from reactive oxygen intermediates (ROI) derived from host immune effector cells (21, 32). Therefore, this pigment biosynthesis pathway seems to contribute in a complex manner to the pathogenicity of *A. fumigatus*. Melanins are pigments of high molecular weight that are formed by oxidative polymerization of phenolic and/or indolic compounds with free radical-generating and -scavenging activity (42). They protect the fungus from oxidants (20), extreme temperatures (43), UV light (53), heavy metals (13, 14, 19), and antifungal agents (17). Previously, it was shown that melanins play an important role in the virulence of a broad range of pathogenic fungi (reviewed in references 19, 32, 37, and 49). Many fungi are able to synthesize black or brown pigments derived from L-tyrosine via dihydroxyphenylalanine (DOPA) (37, 55) in addition to DHN melanin. The DOPA-melanin pathway, in which tyrosinases or laccases hydroxylate tyrosine via DOPA to dopaquinone, which then auto-oxidizes and polymerizes, is the best-characterized melanization pathway from L-tyrosine (32). However, brown pigments may also be produced from L-tyrosine via a pathway involving the accumulation and auto-oxidation of intermediates of tyrosine catabolism (6, 7, 28). For instance, pyomelanins are synthesized from tyrosine through *p*-hydroxyphenylpyruvate (PHPP) and homogentisic acid (HGA) (7). The tyrosine degradation pathway has been subject to investigations in humans, as many severe metabolic disorders, e.g., phenylketonuria, alkaptonuria, tyrosinemia, and Hawkinsinuria, are associated with enzymatic defects in catabolism of phenylalanine and tyrosine (10, 35, 40). The genetic and biochemical basis of the inherited disorder alkaptonuria was elucidated largely by elegant experiments with the important

* Corresponding author. Mailing address: Department of Molecular and Applied Microbiology, Leibniz Institute for Natural Product Research and Infection Biology, Hans Knöll Institute and Friedrich Schiller University Jena, Beutenbergstrasse 11a, 07745 Jena, Germany. Phone: 49 (0)3641-532 1001. Fax: 49 (0)3641-532 0802. E-mail: axel.brakhage@hki-jena.de.

† J.S.-R. and V.S. contributed equally to this work.

‡ Present address: Department of Medical Microbiology and Hospital Hygiene, University Hospital Rostock, Schillingallee 70, 18057 Rostock, Germany.

▽ Published ahead of print on 21 November 2008.

TABLE 1. Fungal strains used in this study

Strain	Description	Reference
CEA17Δ*akuB*^{KU80}	*akuB*^{KU80}::*pyrG*; PyrG^{+}	8
Δ*hmgA* mutant	*akuB*^{KU80}Δ; *hmgA*::*ptrA*; PtrA^{r}	This study
Δ*hppD* mutant	*akuB*^{KU80}Δ; *hppD*::*ptrA*; PtrA^{r}	This study
hmgA^{C} mutant	*akuB*^{KU80}Δ; *hmgA*Δ::*hmgA*	This study
hppD^{C} mutant	*akuB*^{KU80}Δ; *hppD*Δ::*hppD*	This study
pksP mutant	Contains a nonfunctional *pksP* gene	30
Δ*abr2* mutant	*abr2*Δ::*hph*, derived from ATCC 46645, Hyg^{r}	47

TABLE 2. Oligonucleotides used in this study

Oligonucleotide	Sequence (5′→3′)
HmgAXbaI_for	ACCAGTCATTCATCTAGACGACGCC
HmgAXbaI_rev	CATCCGTGACTCTAGAGCATCATCC
HmgASfiI_up	AGGCCTGAGTGGCCGGCATGACGTCGAATATCTGC
HmgASfiI_down	AGGCCATCTAGGCCCCAACAAGGCCTAGTAGGAAG
HppD_for	CATCTCCTCCAGTTGATCGG
HppD_rev	TTCTCTCAACATGACTGTCACC
HppD_SfiI_up	AGGCCTGAGTGGCCATAAGAGCTGTCAGAGAGGC
HppD_SfiI_down	AGGCCATCTAGGCCCTTGTATAGGACTTCGGTGC
hmgA_FspI_for	CACAACGTCATGAGTGCGCATGGTCCCGAC
hmgA_FspI_rev	GTCGGGACCATGCGCACTCATGACGTTGTG
HppD*_C_for	CCTCAAGGCTCGAGGTGTTGAG
HppD*_C_rev	CTCAACACCTCGAGCCTTGAGG
AfCitAcode_up	GCAAGGTCATCGGCGAGG
AfCitAcode_down	GTTGTCACCGTAGCCGAGC
AfHppDcode2_for	TGCGCAACGGCGACATCAC
AfHppDcode2_rev	TGGCGGGTTCGTTGATGGG
AfHmgAcode_up	ACCTGCTGGAAGGGTGACAC
AfHmgAcode_down	ACCAGACTGGCTTCGACTCC

model organism *Aspergillus nidulans* (11, 40). Pyomelanin and alkaptomelanin are merely different designations for the same pigment. However, the pigment produced by microbes is often referred to as pyomelanin, and the pigment produced by humans is called alkaptomelanin. The term pyomelanin was first introduced by Yabuuchi and Ohyama, who described a water-soluble brown pigment produced by the sanious bacterium *Pseudomonas aeruginosa* (56).

Although the synthesis of pyomelanin in a broad range of bacteria has been postulated, little is known about the tyrosine degradation pathway via HGA in clinically important fungi. Here, we showed for the first time that *A. fumigatus* is able to produce pyomelanin from L-tyrosine via HGA. We analyzed its biochemical and genetic basis.

MATERIALS AND METHODS

Strains and culture conditions. *A. fumigatus* strains used in this study are listed in Table 1. Strain CEA17Δ*akuB*^{KU80} (8) was used as the wild type, unless otherwise noted, and to generate the Δ*hmgA* and Δ*hppD* deletion strains. *A. fumigatus* was cultivated in *Aspergillus* minimal medium (AMM) as described previously (54), containing 2% (wt/vol) agar for solid medium. Unless otherwise noted, 50 mM glucose was used as the carbon source. Liquid cultures were always grown at 37°C with shaking at 200 rpm. Pyrithiamine (Sigma-Aldrich, Germany) in a final concentration of 0.1 μg ml^{-1} was added when selection for pyrithiamine resistance was required. For inhibition of HppD, sulcotrione (Riedel-de Haën, Germany) was used in a final concentration of 50 μmol liter^{-1}. For propagation of plasmids, *Escherichia coli* α-Select chemically competent cells (Bioline, Germany) were employed and cultivated at 37°C in LB medium, supplemented with 100 μg ml^{-1} ampicillin or 50 μg ml^{-1} kanamycin.

Standard DNA techniques. Standard techniques for manipulation of DNA were carried out as described previously (45). Chromosomal DNA of *A. fumigatus* was prepared using a Master pure yeast DNA purification kit (Epicentre Biotechnologies). Southern blot analysis was carried out as previously described (16).

Two-dimensional gel electrophoresis. *A. fumigatus* wild-type strain ATCC 46645 was preincubated for 14 h in AMM and further incubated for 55 h with and without the addition of 10 mM L-tyrosine. Proteome analysis of *A. fumigatus* mycelium extracts was essentially carried out according to the method described in reference 26. The absolute amount of 150 μg of protein was applied via anodic cup loading to rehydrated immobilized pH gradient strips with a nonlinear pH gradient from 3 to 11 (GE Healthcare Bio-Sciences, Germany). The second-dimension electrophoresis was performed with an Ettan DALTsix system (GE Healthcare Bio-Sciences, Germany). Preparative gels for mass analysis were stained with colloidal Coomassie blue (36), and for quantitative analysis, spots were made visible with a PlusOne silver staining kit (GE Healthcare Bio-Sciences). Images were analyzed with Image Master Platinum software (version 5.0). After background subtraction and normalization, spots were quantified using percent spot volumes, ratios, and gap parameters. Protein spots of interest were cut out and tryptically digested (47). Peptide mass and peptide fragment fingerprint spectra were measured by matrix-assisted laser desorption ionization–time of flight/time of flight mass spectrometry (Ultraflex 1; Bruker Daltonics, Germany) and subsequently identified by searching the fungi section of the NCBI database using the MASCOT interface (MASCOT 2.1.03; Matrix Science, United Kingdom) with the following parameters: Cys as an *S*-carbamidomethyl derivative and Met in oxidized form (variable), one missed cleavage site, and a peptide mass tolerance of 200 ppm. Hits were considered significant according to the MASCOT score ($P < 0.05$).

Generation of deletion mutants. DNA fragments were amplified with Phusion high-fidelity DNA polymerase (Finnzymes, Finland) or Extender Polymerase Systeme (5 PRIME, Germany). To generate the *hmgA* knock-out plasmid, the *hmgA* gene, including 1.2-kbp upstream and downstream flanking regions, was amplified by PCR using oligonucleotides HmgAXbaI_for and HmgAXbaI_rev, introducing XbaI restriction sites (Table 2). The PCR product was cloned into plasmid pCR2.1 (Invitrogen, Germany), yielding pCR2.1*hmgA*. After digestion with XbaI, the 3,867-bp product was isolated and ligated into the single XbaI restriction site of plasmid pUC18 (Fermentas, Germany). The resulting plasmid, pUC18*hmgA*, was used as the template for an inverse PCR, employing the primers HmgASfiI_up and HmgASfiI_down, both containing an SfiI restriction site. Ligation of the SfiI-digested PCR fragment resulted in the generation of plasmid pUCΔ*hmgA*. The pyrithiamine resistance gene (*ptrA*) from plasmid pSK275 (gift from S. Krappmann), conferring pyrithiamine resistance (29), was inserted into the SfiI restriction site to yield pUC18Δ*hmgAptrA*. The Δ*hmgAptrA* sequence was amplified by PCR using oligonucleotides HmgAXbaI_for and HmgAXbaI_rev. The obtained PCR product was used for transformation of *A. fumigatus*. For deletion of the *hppD* gene, plasmid pCR2.1Δ*hppDptrA* was generated. The *hppD* gene, including upstream and downstream flanking regions, was amplified from *A. fumigatus* genomic DNA using the oligonucleotides HppD_for and HppD_rev. The resulting 3,660-bp DNA fragment was cloned into plasmid pCR2.1. This plasmid was used as the template for the amplification with oligonucleotides HppD_Sfi_up and HppD_Sfi_down to modify the ends of the flanking regions with SfiI restriction sites and to remove the *hppD* coding sequence. After SfiI digestion of the PCR product, the *ptrA* gene was inserted as an SfiI fragment to give plasmid pCR2.1Δ*hppDptrA*. PCR was performed employing pCR2.1Δ*hppDptrA* as the template and oligonucleotides HppD_for and HppD_rev. The resulting DNA fragment, containing the *ptrA* gene flanked by *hppD* upstream and downstream regions, was used for transformation of *A. fumigatus*. Transformation of *A. fumigatus* was carried out using protoplasts as described previously (54).

Complementation of Δ*hmgA* and Δ*hppD* mutants. The Δ*hmgA* and Δ*hppD* mutant strains were complemented at the original gene locus by the use of modified wild-type genes. A dominant selection marker was not required, since Δ*hmgA* and Δ*hppD* mutant strains did not sporulate on AMM agar plates when L-tyrosine or L-phenylalanine was used as the sole carbon source. To distinguish between wild-type and complemented strains in Southern blot analysis, the nucleotide sequences of *hppD* and *hmgA* were slightly modified without affecting the protein sequence (see Results). To complement the Δ*hmgA* mutant with the *hmgA* sequence, plasmid pUC*hmgA*^{C} was generated. In this plasmid, an addi-

tional FspI restriction site was introduced into the *hmgA* gene by PCR by employing a FlipFlop site-directed mutagenesis kit (Bioline, Germany) with the help of oligonucleotides hmgA_FspI_for and hmgA_FspI_rev. For transformation of the *A. fumigatus* Δ*hmgA* strain, a PCR fragment was generated, using pUC*hmgA*^{C} as the template and oligonucleotides HmgAXbaI_for and HmgAXbaI_rev. To complement the deletion of the Δ*hppD* strain, plasmid pCR2.1*hppD*^{C} was generated. In this plasmid, an additional XhoI restriction site was introduced into the *hppD* sequence by employing a FlipFlop site-directed mutagenesis kit and oligonucleotides HppD*_C_rev and HppD*_C_for the *A. fumigatus* Δ*hppD* strain was transformed with a DNA fragment obtained by PCR with pCR2.1*hppD*^{C} as the template and oligonucleotides HppD_rev and HppD_for.

Susceptibility to H_2O_2 and diamide. The sensitivities of the mutant strains to H_2O_2 and diamide compared with those of the wild-type strain were measured by agar plate diffusion assays. The 25-ml top and 25-ml bottom agar consisted of AMM supplemented with 50 mM glucose and 20 mM L-tyrosine. Conidia (2.5×10^8) were added to the top agar and poured on top of the bottom agar in a petri dish. When the susceptibility of fresh conidia was tested, the oxidative insult was added immediately. To test the effect of H_2O_2 and diamide on germlings, agar plates were preincubated for 10 h at 37°C before the addition of the reagent. For both approaches, 150 μl of 5% (vol/vol) H_2O_2 or 200 μl of 0.2 M diamide was added via a hole with a diameter of 10 mm which was punched in the middle of the agar. Inhibition zones were measured 22 h after addition of the oxidative reagent. Eight replicates from three independent experiments served for the calculation of means and standard deviations.

Homogentisate dioxygenase assay. HmgA activity was determined spectrophotometrically by measuring the formation of maleylacetoacetate at 330 nm as previously described (12). In brief, crude extracts were prepared from mycelia grown in liquid media. Conidia (1×10^7) were inoculated in 100 ml AMM. After 20 h of preincubation, L-tyrosine was added, if necessary, to a final concentration of 10 mM. After a further 23 h of incubation, mycelia were harvested and either frozen in liquid nitrogen and stored or directly lysed by sonication in 50 mM potassium phosphate buffer, pH 7. After 15 min of centrifugation at 13,000 × *g*, the supernatant was used for enzyme assays containing 50 mM potassium phosphate buffer (pH 7), 2 mM ascorbate, 50 μM $FeSO_4$, 200 μM HGA, and crude protein extract at a concentration of 50 μg/ml. The substrate, HGA, was added just before measurement and after preincubation of the assay mixture for 10 min at 20°C. Homogentisate dioxygenase activity was calculated using the molar extinction coefficient of maleylacetoacetate, 13,500 M^{-1} cm^{-1} (46). Protein concentrations for calculation of specific activities were determined using a Coomassie Plus protein assay (Pierce Biotechnology).

FTIR analysis. AMM (100 ml) with 50 mM glucose and 10 mM L-tyrosine was inoculated with 3×10^8 *A. fumigatus* Δ*hmgA* conidia. After cultivation for 53 h, the supernatant was filtered with Miracloth (Calbiochem) and precipitated overnight at room temperature by adjusting the pH to 2.0 with 1 M HCl. After centrifugation (16,100 × *g*, 20 min), the pellet was resuspended in 2.5 ml water at pH 12 and dialyzed in 3.5-kDa Slide-A-Lyzer dialysis cassettes (Pierce Biotechnology) against water, accompanied by a stepwise reduction of the pH from 10 to 7. The lyophilized pigment was then used for Fourier transform infrared spectroscopy (FTIR) analyses. In vitro-synthesized pyomelanin was used as the control in FTIR spectroscopy. Synthetic pyomelanin was produced by autooxidation of a 10 mM HGA solution at pH 10 with constant stirring for 3 days (adapted from reference 44). Polymerization was stopped, and precipitation was started by adjusting the pH to 2 with 6 M HCl. After precipitation overnight and centrifugation (16,100 × *g*, 20 min), the pellet was resuspended in 2.5 ml water at pH 12 and further treated as described above. The lyophilized sample was used for FTIR spectroscopy. Synthetic pyomelanin and melanin prepared from in vitro cultures were analyzed by using KBr disks with an FTIR spectrophotometer (FT/IR-4100; Jasco) equipped with a deuterated L-alanine triglycine sulfate detector.

Melanin formation and analysis of *A. fumigatus* cultures. AMM (200 ml) was inoculated with 1×10^7 conidia of each respective *A. fumigatus* strain. After 20 h of preincubation, L-tyrosine was added to a final concentration of 10 mM. Every 4 h, 4-ml samples were taken and filtered through Miracloth. Aliquots were stored at −20°C for further analyses. Pigment formation was analyzed by direct absorbance measurements of the supernatant of an alkalized (20 μl of 5 M NaOH per ml of sample) and centrifuged (16,000 × *g* for 2 min) sample at 405 nm. Another aliquot was acidified (20 μl of 10 M HCl per ml of sample), and the glucose concentration was determined by a chip sensor device (BIOSEN C_line, package GP+; EKF-diagnostic GmbH, Germany). Samples for HPLC were additionally filtered through Millex-LCR_{13} filter units (0.5 μm; Millipore). Twenty microliters of the sample was injected into a Shimadzu high-pressure liquid chromatography (HPLC) system fitted with an RP_{18} column (Eurospher 100C18, 250 mm by 4.6 mm, 5 μm; Merck, Germany). For elution, water with 0.1% (vol/vol) trifluoroacetic acid was used as buffer A and acetonitrile with 0.1% (vol/vol) trifluoroacetic acid was used as buffer B. Peaks were eluted at a flow rate of 1 ml min^{-1} by applying the following gradient: 8% B for 12 min, gradient from 8% B to 95% B within 3 min, 95% B for 1 min, gradient from 95% B to 8% B within 2 min and, finally, 5 min at 8% B for recalibration. The compounds were detected with a Shimadzu LC-10 AD diode array detector at 280 nm. L-Tyrosine and HGA eluted under these conditions at 7.7 and 8.6 min, respectively. Concentrations of L-tyrosine and HGA were determined by calculations of peak areas at 280 nm and comparisons with standard curves for L-tyrosine and HGA, respectively. For instrument control, data acquisition, and data analysis, the CLASS-VP package (Shimadzu GmbH, Germany) was employed.

RNA isolation and first-strand cDNA synthesis. For RNA isolation from in vitro-grown cultures, *A. fumigatus* was cultivated with and without 10 mM L-tyrosine as described for the homogentisate dioxygenase assay. Mycelium (100 mg) was used for RNA extraction employing a MasterPure yeast RNA purification kit (Epicentre Biotechnologies). After DNase treatment, 10 μg of total RNA was used for first-strand cDNA synthesis with SuperScript III reverse transcriptase and anchored oligo$(dT)_{20}$ primers (Invitrogen, Germany). Reverse transcription was conducted at 50°C for 3 h. RNA was hydrolyzed with 15 μl of 1 M NaOH for 10 min at 70°C and subsequently neutralized with 15 μl of 1 M HCl. After the addition of 6 μl of 3 M sodium acetate (pH 5.2), 2.5 μl of glycogen (5 mg/ml), and 200 μl of ice cold ethanol, cDNA was precipitated overnight at −20°C. After centrifugation for 30 min at 4°C and 16,000 × *g*, the pellet was washed with 70% (vol/vol) ethanol and resolubilized in 30 μl of Tris-HCl buffer, pH 8.0.

Reverse transcription-PCR analysis. cDNA synthesis was used to determine transcription levels of *hmgA* and *hppD* compared with those of the constitutively formed citrate synthase (Afu5g04230, *citA*) transcripts according to the method described in reference 18. For this purpose, oligonucleotides AfCitAcode_up and AfCitAcode_down were used for the amplification of a 575-bp fragment of *citA* transcripts. Oligonucleotides AfHppDcode2_for and AfHppDcode2_rev allowed the specific amplification of a 591-bp region of *hppD* transcript. With oligonucleotides AfHmgAcode_up and AfHmgAcode_down, a 563-bp DNA fragment of the coding region of *hmgA* could be detected. Transcript amplification using GoTaq DNA polymerase (Promega, Germany) was carried out with a Veriti fast thermal cycler (Applied Biosystems) with 5 ng cDNA isolated from in vitro-grown cultures as the template. As the control, 0.1 ng genomic DNA was applied under the same conditions.

RESULTS

Addition of L-tyrosine leads to the production of a pyomelanin in *A. fumigatus* catalyzed by the tyrosine degradation pathway. *A. fumigatus* produced a brown pigment when grown in AMM supplemented with L-tyrosine. This brown compound accumulated in the hyphae but was also excreted into the medium (Fig. 1A). Since *A. fumigatus* is known to produce DHN melanin (22, 30, 51), we tested whether the biosynthesis of the pigment is connected to that of DHN melanin. Therefore, two *A. fumigatus* mutant strains deficient in DHN melanin biosynthesis were analyzed. The *A. fumigatus pksP* mutant strain produces white conidia due to a mutation in the PksP polyketide synthase that is essential for DHN melanin biosynthesis (30). The Δ*abr2* strain also has a defect in DHN melanin biosynthesis due to deletion of a laccase (48). Interestingly, both DHN melanin mutant strains, the *pksP* mutant and the Δ*abr2* strain, were able to produce the brown pigment induced by the addition of L-tyrosine to the medium (see Fig. 3D for the *pksP* mutant phenotype), excluding the possibility that the brown pigment represented some DHN melanin derivative.

Proteome analysis applying two-dimensional gel electrophoresis of mycelia grown in the presence of tyrosine (Fig. 1B) led to the identification of proteins that were assigned to tyrosine catabolism (Table 3, shown in bold). These proteins were candidates likely to be involved in the degradation of L-tyrosine to HGA that

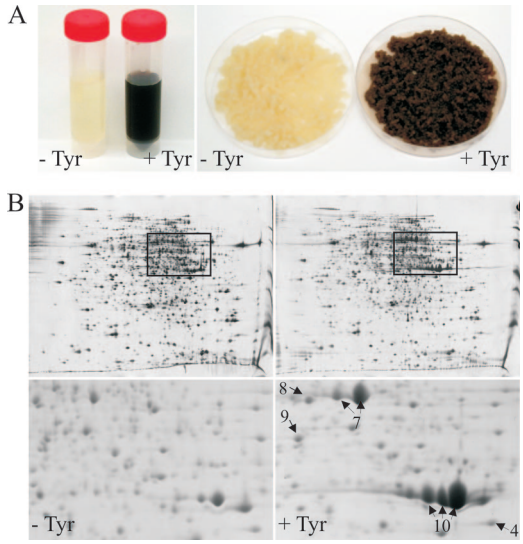

FIG. 1. Pigment formation and proteome analysis of *A. fumigatus* grown with (+Tyr) and without (−Tyr) L-tyrosine. The wild-type strain was preincubated for 15 h in AMM and then further incubated for 55 h with and without the addition of 10 mM L-tyrosine. (A) Pigment formation was observed for *A. fumigatus* mycelia and in the medium. (B) Two-dimensional gel electrophoresis of proteins extracted from *A. fumigatus* hyphae. Silver-stained protein pattern of cytoplasmic proteins from *A. fumigatus* grown with and without the addition of 10 mM L-tyrosine. Selected protein spots with increased levels are highlighted by numbered arrows. They correspond to the proteins listed in Table 3.

can polymerize to pyomelanin (Fig. 2A). By a BLAST search of the TIGR database (http://www.tigr.org/tdb/e2k1/afu1/), the genes putatively involved in tyrosine degradation were deduced from the identified proteins. Aspartate transaminase catalyzes the deamination of L-tyrosine to *p*-hydroxyphenylalanine. The tyrosine degradation product fumarate can be introduced into the citrate circle, where it is metabolized to oxaloacetate via malate dehydrogenase after conversion to malate by fumarate hydratase, which explains the upregulation of malate dehydrogenase. The other two identified genes form a cluster with four further genes (Fig. 2B). Database annotations predicted three introns for both the *hppD* and *hmgA* genes. It is interesting that the AFUA_2g04210, *fahA*, and *maiA* genes apparently do not contain any introns. The AFUA_2g04210 gene encodes a conserved hypothetical protein of unknown function. A putative transcription factor containing a fungal Zn_2Cys_6 binuclear cluster domain (AFUA_2g04262) is located 1,071 bp upstream of the *maiA* gene. The gene cluster shows similarity to the respective cluster in *A. nidulans*, which was shown to be involved in tyrosine degradation (11). However, in *A. nidulans*, there is an additional putative gene (AN 1894.3) of unknown function between the gene encoding a putative transcription factor (AFUA_2g04262) and the maleylacetoacetate isomerase gene, which is absent in the *A. fumigatus* genome. The other upregulated proteins, NADH-quinone oxidoreductase, glyceraldehyde 3-phosphate dehydrogenase, aldehyde dehydrogenase, and alcohol dehydrogenase, may also be involved in tyrosine metabolism. Nucleoside diphosphate kinase and peptidyl-prolyl *cis-trans* isomerase are rather unspecifically upregulated due to secondary effects.

Deletion of *hppD* and *hmgA* impairs growth on L-tyrosine as the sole carbon source and affects pyomelanin formation. To verify the predicted pathway and to analyze the effect of accumulation of HGA on the pigment formation of *A. fumigatus*, the two central genes of the pathway, *hmgA* and *hppD*, were deleted. HppD catalyzes the formation of HGA, whereas homogentisate dioxygenase is involved in the cleavage of the aromatic ring of HGA and its conversion to maleylacetoacetate (Fig. 2A). For deletion of *hmgA* and *hppD* in *A. fumigatus*, the coding sequence of each gene was replaced by *ptrA*. For complementation of the deletion mutants, a strategy based on homologous recombination was applied using the wild-type gene in which a point mutation was inserted. In the *hmgA* gene, thymine at position 1248 was replaced by guanine. This base exchange did not alter the amino acid sequence but introduced an FspI restriction site that enabled differentiation between wild-type and complemented mutant strains by Southern blot analysis. For complementation of the *hppD* gene, cytosine at position 1022 was replaced by thymine, introducing an XhoI restriction site. Selection of complemented strains was achieved by using AMM agar plates containing phenylalanine as the sole carbon source. After transformation, complemented strains were able to produce conidia, in contrast to the deletion strains with phenylalanine as the sole carbon source, which did not sporulate (data not shown; see Fig. 3C).

The integration of the *ptrA* gene in the locus of the *hppD* and *hmgA* genes and the reintroduction of wild-type genes are shown in Fig. 3A and B. In the *hmgA* mutant strain, the band

TABLE 3. Proteins with increased levels in *A. fumigatus* cultures grown in AMM after supplementation with 10 mM L-tyrosine

Spot no.[a]	Protein name[c]	Sequence coverage (%)	Mascot score[b]	Protein molecular mass (kDa)	Accession no.
1	NADH-quinone oxidoreductace Pst2	64	1,117	21.8	gi:66847664
2	Nucleoside diphosphate kinase	68.6	87	16.9	gi:70984978
3	Peptidyl-prolyl *cis-trans* isomerase/cyclophilin	42.9	73.4	17.7	gi:66852503
4	**Malate dehydrogenase, NAD dependent**	61.8	165	35.9	gi:70986899
5	Glyceraldehyde 3-phosphate dehydrogenase	39.1	111	36.4	gi:70985278
6	**Aspartate transaminase**	58.2	187	51.2	gi:66852936
7	Aldehyde dehydrogenase	57.4	165	54.7	gi:70982606
8	**Homogentisate 1,2-dioxygenase**	43.7	126	50.2	gi:70989409
9	**Fumarylacetoacetate hydrolase**	41.3	132	46.8	gi:70989411
10	Alcohol dehydrogenase	70	165	37.9	gi:70982604

[a] Spot number according to Fig. 1B.
[b] Mascot score represents the probability that the observed match is a random event. Only protein scores with P values of <0.05 were considered significant.
[c] Proteins in bold are involved in tyrosine metabolism via HGA.

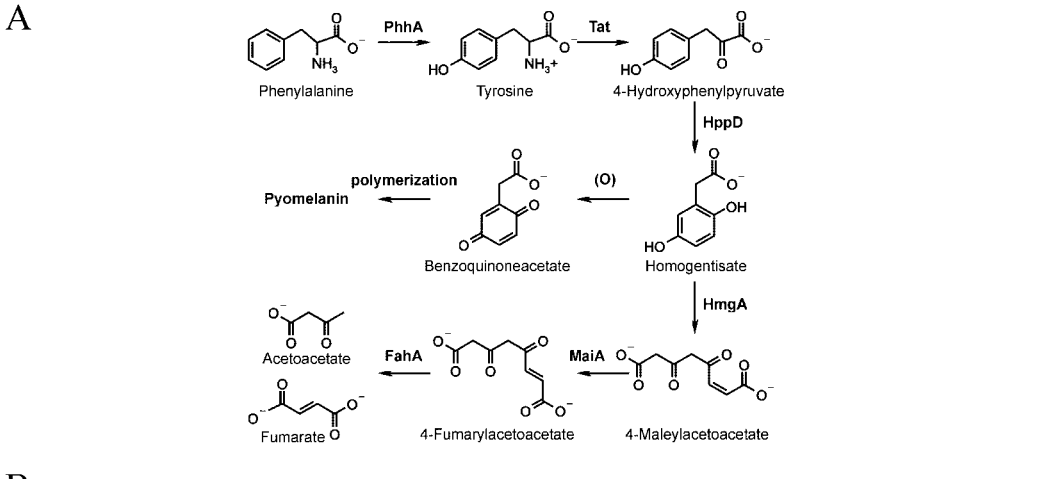

Locus tag	Gene	Transcript size	Introns	Gene Product	Deduced protein size
AFUA_2G04200	*hppD*	1212	3	4-hydroxyphenylpyruvate dioxygenase	404
AFUA_2G04210		771	0	conserved hypothetical protein	257
AFUA_2G04220	*hmgA*	1350	3	homogentisate dioxygenase	450
AFUA_2G04230	*fahA*	1296	0	fumarylacetoacetate hydrolase	432
AFUA_2G04240	*maiA*	696	0	maleylacetoacetate isomerase	232
AFUA_2G04262		2247	3	C6 transcription factor, putative	749

FIG. 2. (A) L-Tyrosine degradation pathway (modified from reference 35). The enzymes involved are indicated in bold as follows: PhhA, phenylalanine hydroxylase; Tat, tyrosine aminotransferase; HppD, 4-hydroxyphenylpyruvate dioxygenase; HmgA, homogentisate dioxygenase; MaiA, maleylacetoacetate isomerase; FahA, fumarylacetoacetate hydrolase. Homogentisate can lead to the production of pyomelanin through benzoquinone acetic acid after oxidation (O) and polymerization. (B) Organization of the L-tyrosine degradation gene cluster in *A. fumigatus*. Genes are illustrated as arrows. Locus tags, transcript sizes, numbers of introns, putative protein function, and the number of amino acids of the deduced proteins are listed.

of 4.5 kbp, characteristic of the wild type, had disappeared. Instead, an 8.2-kbp DNA fragment was visible, indicative of the *ptrA*-encoding DNA fragment and thus the replacement of the wild-type gene with the *ptrA* gene. In the *hmgA* complemented strain, the expected band of 2.1 kbp was visible. The *hmgA* deletion strain and the complemented strain were designated the Δ*hmgA* and *hmgA*^{C} strains, respectively. In the *hppD* deletion strain, the band at 2.2 kbp, which is characteristic of the wild-type strain, had disappeared. Instead, the fragment at 3.6 kbp appeared. In the complemented strain, only the characteristic fragment at 1.5 kbp was detectable. These strains were referred to as the Δ*hppD* and *hppD*^{C} strains in further studies. The phenotypes of the Δ*hmgA* and Δ*hppD* strains were characterized with different media (Fig. 3C). On AMM agar plates, no differences in growth of the deletion strains and wild-type strains were apparent (Fig. 3C, left panel). The addition of 10 mM L-tyrosine to AMM liquid cultures (Fig. 3D) stained the mycelia and culture media of wild-type, complemented, and *pksP* mutant strains light brown, whereas in the Δ*hmgA* mutant, the color was dark brown. In contrast, no pigment production was observed for the Δ*hppD* strain. An examination of pigment release in liquid cultures (Fig. 3E) indicated that besides tyrosine, phenylalanine and phenylacetate also provoke pigment formation. Tyrosine addition led to the highest pigment formation in wild-type cultures, which is the reason tyrosine was used in most experiments as the inducer. Furthermore, when tyrosine was given as the sole carbon source, the growth rate of the Δ*hppD* strain was reduced on agar plates, the mycelia of the Δ*hppD* and Δ*hmgA* strains were less dense, conidiation was severely impaired, and tyrosine crystals in the media were not consumed, in contrast to observations for wild-type and complemented strains (Fig. 3C). Still, the pigment was clearly visible in the Δ*hmgA* deletion strain due to residual mycelial growth based on carbon sources present in the agar. The same was true for the growth on L-phenylalanine as the sole carbon source (data not shown). The severe growth defects on AMM agar plates with tyrosine or phenylalanine as the sole carbon source confirmed the involvement of HmgA and HppD in tyrosine degradation.

Additionally, the strains were incubated on AMM agar plates supplemented with HGA or PHPP. The addition of

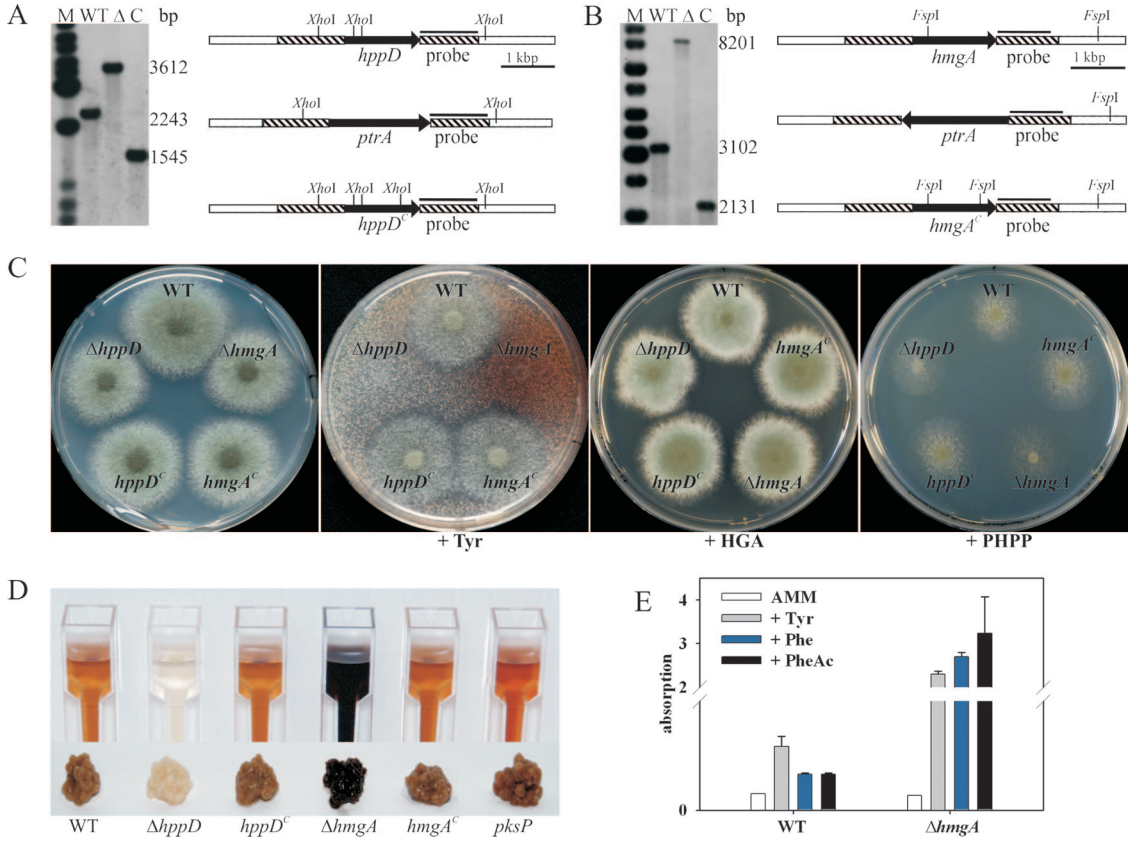

FIG. 3. (A and B) Deletion and complementation of *hppD* and *hmgA*. (A) Schematic representation of the chromosomal *hppD* locus in the wild type (WT), the *hppD* deletion mutant (Δ), and the complemented (C) strain. Southern blot analysis proves the deletion of the *hppD* gene and the reintroduction of the point mutation-carrying *hppD* gene containing an additional XhoI restriction site. M denotes the lane with the Gene Ruler 1-kb DNA ladder (Fermentas, Germany). (B) Schematic representation of the chromosomal *hmgA* locus in the WT, the *hmgA* deletion mutant (Δ), and the complemented (C) strain. Southern blot analysis verified the deletion of the *hmgA* gene and the reintroduction of the point mutation-carrying *hmgA* gene with an extra FspI site. Lane M depicts HyperLadder I (Bioline GmbH, Germany). Restriction endonuclease cleavage sites, the DNA fragments identified by Southern blot analysis, and the positions to which the probe hybridizes are indicated. (C) Phenotypes of the wild-type (WT), Δ*hmgA*, Δ*hppD*, and complemented mutant strains grown for 68 h on AMM agar plates with 50 mM glucose (left panel) and without glucose but with 10 mM L-tyrosine as the sole carbon source. The growth on AMM agar plates with 50 mM glucose and 10 mM PHPP or, alternatively, 10 mM HGA is also shown. (D) Pigment production of wild-type, Δ*hmgA*, Δ*hppD*, complemented, and *pksP* mutant strains grown in AMM with L-tyrosine. The strains were cultivated for 64 h in 50 ml of AMM supplemented with 10 mM L-tyrosine and with an inoculum of 5×10^7 conidia. The upper panel displays the culture permeates and the lower panel the mycelia. (E) Quantification of pigment production by absorption measurements at 405 nm. CEA17Δ*akuB*^{KU80} wild-type and Δ*hmgA* mutant strains were inoculated with 1×10^5 conidia/ml for 68 h in AMM (white bar), AMM with 10 mM L-tyrosine (gray bar), AMM with 10 mM L-phenylalanine (blue bar), and AMM with 10 mM phenylacetate (black bar). The experiment was repeated three times in duplicate. Standard deviations are calculated from two independent experiments.

HGA, the accumulation product of the Δ*hmgA* strain, did not impair growth; therefore, pyomelanin formation is not a result of detoxification of HGA. However the addition of PHPP, the accumulation product of the Δ*hppD* mutant, led to reduced growth and sporulation of the wild-type strain, even more so with the deletion strains. Consequently, PHPP needs to be degraded for detoxification. Integration of a functional gene cured the defects of the deletion strains on all applied media, demonstrating that the phenotypes are a direct result of the loss of HmgA and HppD activity.

Pigment results from polymerization of HGA. FTIR spectroscopy was used to analyze the pigment, which accumulated in cultures of the Δ*hmgA* strain, since it is regarded as the most informative method for structural analysis of melanins (3). The overlay of the FTIR spectra of synthetic pyomelanin and pigment extracted from fungal cultures showed a high degree of similarity (Fig. 4). Both spectra depict a broad absorption at 3,420 cm^{-1}, which is due to associated or polymeric OH groups. The stretching vibrations for aliphatic CH bonding appear at 2,952 cm^{-1} and 2,925 cm^{-1} for natural and synthetic melanin, respectively. At 1,586 cm^{-1}, the symmetric carboxylate stretching vibrations (COO^-) are detectable according to the basic isolation procedure. The fingerprint regions between 1,450 cm^{-1} and 650 cm^{-1} resemble each other closely. The high level of identity between the synthetic pyomelanin and the pigment extracted from fungal cultures indicates that the Δ*hmgA* mutant produces pyomelanin when cultivated with L-tyrosine.

HGA accumulation correlates with L-tyrosine consumption and pyomelanin formation. To provide evidence for pigment formation from L-tyrosine via the accumulation of HGA, ty-

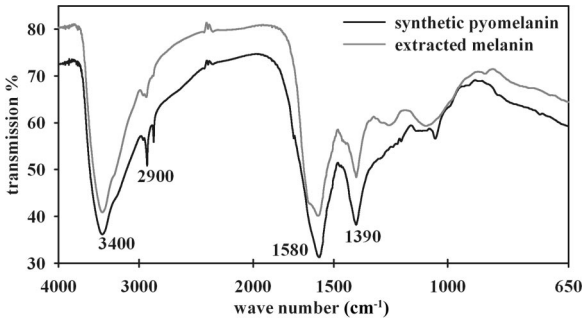

FIG. 4. FTIR spectrum overlay from synthetic HGA melanin and lyophilized extracellular pigment extracted from Δ*hmgA* culture.

rosine catabolism in *A. fumigatus* liquid cultures was analyzed. Melanin accumulation was observed by measuring absorption at 405 nm. L-Tyrosine and HGA concentrations were determined by HPLC analysis. In cultures grown without L-tyrosine, pigment accumulation and HGA formation were lacking (Fig. 5A). For wild-type and Δ*hmgA* AMM tyrosine cultures, the consumption of L-tyrosine and the formation of HGA were clearly visible (Fig. 5B and E). In the Δ*hmgA* strain, HGA concentration as well as absorption values were even higher than those of the wild type. In this mutant, HGA accumulated because HGA could not be cleaved to maleylacetoacetate (Fig. 2A). Δ*hmgA* cultures showed a decelerated decrease in L-tyrosine concentration, probably due to a feedback inhibition via accumulation of HGA. The analysis of wild-type cultures grown with the HppD inhibitor sulcotrione (9) led to results very similar to those for the Δ*hppD* mutant, i.e., HGA formation was not detected and absorption hardly increased (Fig. 5C and D). Sulcotrione (50 μM) did not inhibit growth of the wild-type strain but prevented formation of pigment when cultivated with 10 mM L-tyrosine.

Additionally, glucose consumption and changes in pH values were monitored. Glucose was completely exhausted after 40 to 50 h of cultivation. An increase in pH was detectable at the same time (Fig. 5F). Therefore, the strains showed very similar growth rates in liquid cultures. This is an important prerequi-

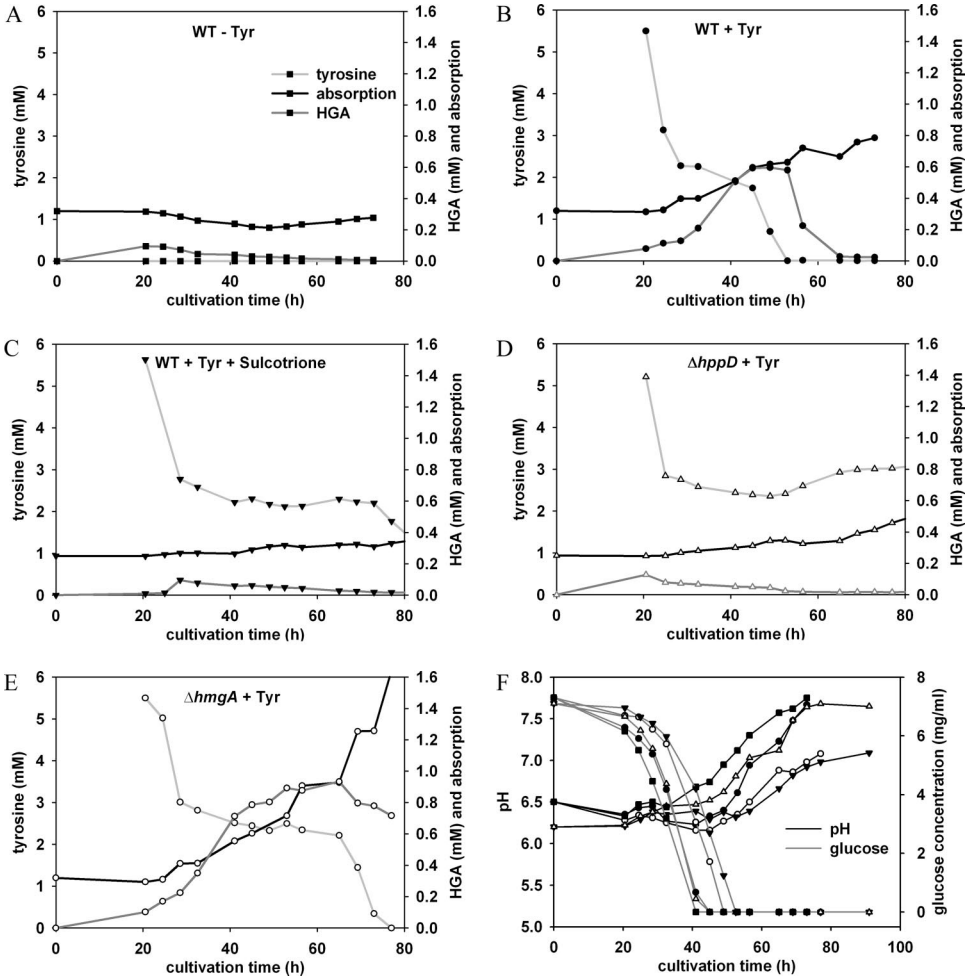

FIG. 5. Pigment formation, HGA synthesis, and L-tyrosine consumption in different *A. fumigatus* strains. The wild type (WT) with (C) and without (B) the Hppd inhibitor sulcotrione and Δ*hppD* (D) and Δ*hmgA* (E) strains were precultivated with 1×10^7 conidia in 200 ml AMM for 20 h prior to the addition of L-tyrosine. Additionally, the wild type was cultivated without tyrosine for comparison (A). Pigment formation is reflected by an increase in absorption at 405 nm. HGA and L-tyrosine concentrations were measured by HPLC. (F) Glucose consumption and pH changes of the cultures mentioned above were monitored.

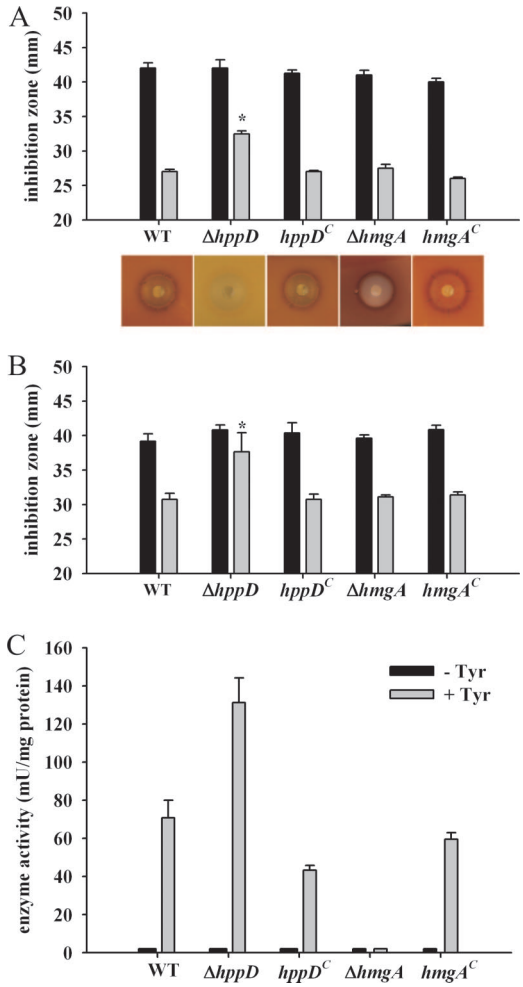

FIG. 6. Sensitivity of Δ*hppD* and Δ*hmgA* mutant strains to H_2O_2 (A) and diamide (B) in an inhibition zone assay. *hppD* and *hmgA* deletion strains were compared with the wild-type (WT) and complemented strains. Black bars indicate the inhibition zones in the assay with fresh conidia, gray bars the inhibition zones with germinated conidia. In all experiments, AMM supplemented with 20 mM L-tyrosine was used. Error bars indicate the standard deviations for three independent experiments with eight replicates. * denotes significantly different ($P < 0.05$) from the wild type. (A) Lower panel, induction of pigmentation on the bottom side in the experiment with preincubation. (C) HmgA activity in Δ*hppD and* Δ*hmgA* mutant strains compared with wild-type and complemented strains. Enzyme-specific activity of mycelia grown with or without 10 mM tyrosine in the medium was determined.

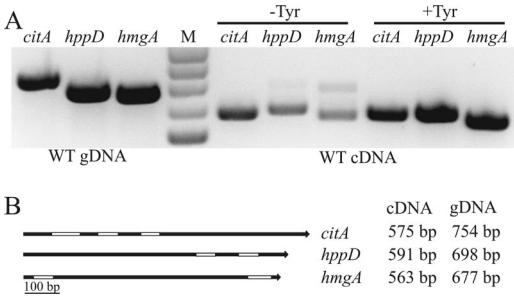

FIG. 7. Semiquantitative analysis of *hmgA* and *hppD* transcripts. (A) Analysis of the wild-type (WT) strain grown in AMM with (+Tyr) and without (−Tyr) the addition of 10 mM L-tyrosine. Lane M, 100-bp DNA ladder; gDNA, genomic DNA; cDNA, first-strand synthesized cDNA; *citA*, transcript of citrate synthase used as the control; *hppD*, transcript of PHPP dioxygenase; *hmgA*, transcript of HGA dioxygenase. *citA* showed a constant mRNA steady-state level and served as the reference for expression levels. (B) Scheme of the expected fragment sizes for *citA*, *hppD*, and *hmgA*. White bars indicate introns. Since the amplified regions from genomic DNA include introns, the PCR products for cDNA are smaller.

site for the analysis of pigment formation, since high pH values accelerate the process and glucose apparently can repress tyrosine catabolism in *Yarrowia lipolytica* (6).

The complemented $hmgA^C$ and $hppD^C$ strains gave the same data as the wild-type strain (data not shown). Taken together, these experiments proved the inability of the Δ*hmgA* strain to degrade HGA and of the Δ*hppD* strain to form HGA. Thus, it was verified that *hppD* and *hmgA* code for 4-hydroxyphenylpyruvate dioxygenase and homogentisate dioxygenase, respectively. Moreover, the data show a positive correlation between HGA accumulation and melanin formation.

Tyrosine catabolism is involved in the oxidative-stress response of *A. fumigatus*. To assess the role of metabolites of the tyrosine degradation in the resistance of *A. fumigatus* to ROI, an agar plate diffusion assay was employed. The sensitivities of Δ*hmgA* and Δ*hppD* mutant strains to H_2O_2 and the thiol-oxidizing agent diamide were compared with those of the wild-type and complemented strains (Fig. 6A and B). The direct confrontation of freshly harvested conidia with both oxidative agents revealed no differences between the strains. To test the sensitivity of germlings, conidia were preincubated for 10 h in AMM before the addition of H_2O_2 and diamide, respectively. Under these conditions, the Δ*hppD* strain showed a significant ($P < 0.05$) increase in ROI sensitivity compared with that of the other strains tested. Pigmentation of hyphae and media was absent only in the Δ*hppD* strain. This finding implies a role of pyomelanin as a protective agent against peroxides and thiol-oxidizing agents. In all strains except for the *hppD* deletion mutant, mycelia were dark colored and melanin was released into the medium (Fig. 6A, lower panel). The pigment accumulated particularly in the border of the inhibition zones, most evidently in the Δ*hmgA* strain assay, which implied a supporting role for H_2O_2 in pigment formation.

Despite the strong pigmentation of the Δ*hmgA* mutant strain, inhibition of growth was comparable to that of the wild-type strain. Consequently, the increase of pigmentation due to the accumulation of HGA in the Δ*hmgA* strain did not further increase resistance to ROI. To confirm that the above-mentioned effects derived from the deletion of the *hmgA* and *hppD* genes, the complemented mutant strains were studied. Both complemented mutant strains revealed inhibition zones similar to that of the wild-type strain in both assays.

Transcription of *hmgA* and *hppD* is induced by tyrosine. A semiquantitative transcript analysis by reverse transcription-PCR allowed the comparison of *hppD* und *hmgA* mRNA steady-state levels of mycelia grown with and without tyrosine. In cultures grown in AMM without L-tyrosine, mRNA steady-state levels of the genes *hppD* and *hmgA* were low in comparison to those of the *citA* reference gene (Fig. 7). In contrast,

the steady-state mRNA level of *hmgA* and *hppD* was strongly increased by the addition of L-tyrosine. This finding correlated well with the increase of HmgA activity upon the addition of L-tyrosine to the medium (Fig. 6C) and shows that the genes are induced by tyrosine at the transcriptional level.

DISCUSSION

One of the characteristics of *A. fumigatus* is the production of gray-green conidia. The pigment consists of a DHN melanin pigment (reviewed in reference 32). Here, we showed for the first time that *A. fumigatus* is able to produce another type of pigment, which was identified by genetic, biochemical, and chemical means as pyomelanin. This compound derived from L-tyrosine via a tyrosine degradation pathway. Further arguments for the presence of this pathway derive from the converse phenotype of the *hppD* mutant compared to a *pksP* mutant deficient in the polyketide synthase essential for DHN melanin formation. The *pksP* mutant strain produced white conidia and released a brown pigment when cultivated with L-tyrosine. In contrast, the Δ*hppD* strain produced pigmented conidia, but no pigment accumulation occurred in liquid cultures supplemented with L-tyrosine. Moreover, the addition of the HppD inhibitor sulcotrione to the medium completely abolished pyomelanin formation by *A. fumigatus*, further confirming that the tyrosine degradation pathway is responsible for pyomelanin formation. The detection of HGA in culture supernatants led to the conclusion that the pigment is synthesized extracellularly and that the darkened mycelia show the deposition of the pigment on the surface of hyphae. Based on these results, *A. fumigatus* has the ability to produce two different melanins, i.e., DHN melanin pigment via the polyketide biosynthesis pathway (30, 51) and pyomelanin via L-tyrosine degradation. DHN melanin was found in many different fungi, both pathogens and nonpathogens (reviewed in references 32 and 55). Until now, pyomelanin has rarely been detected in filamentous fungi. In *A. nidulans*, the pathway was studied to elucidate the molecular basis of inherited diseases of humans involving the formation of black pigments, such as alkaptonuria. Studies of *A. nidulans* and the transfer of results to humans showed that alkaptonuria is associated with enzymatic defects in the catabolism of phenylalanine and tyrosine (10, 40). Studies of an *A. nidulans* Δ*hmgA* deletion mutant (11) bear some analogy to our results with *A. fumigatus*. We focused on the degradation of tyrosine since it is a closer precursor of HGA than phenylalanine and induced stronger pigmentation in the wild-type strain, although the two compounds seem to cause similar effects. As shown for *A. nidulans*, *A. fumigatus* contains only a single functional gene coding for homogentisate dioxygenase. The same is true for PHPP dioxygenase. The pigmentation is induced by tyrosine, phenylalanine, and phenylacetic acid, which agrees well with observations for *A. nidulans*. It will be interesting to compare the regulation of the tyrosine degradation pathway in the two organisms in order to find out whether a basic principle in the difference of virulence of the two strains relies on pyomelanin production. Also, the coexistence of DHN melanin and pyomelanin in *A. fumigatus* (*A. nidulans* does not produce DHN melanin) might be an interesting feature with regard to virulence.

In the thermodimorphic fungus *Paracoccidioides brasiliensis*, which causes paracoccidioidomycosis, genes involved in tyrosine degradation were identified during a microarray analysis. The *hppD* gene was highly expressed during yeast mycelium transition. Addition of an HppD inhibitor inhibited growth and differentiation of the pathogenic yeast phase of the fungus in vitro (39).

The genes *hppD*, *hmgA*, AFUA_2g04210, *fahA*, and *maiA*, which are involved in tyrosine degradation in *A. fumigatus*, form a cluster located on chromosome 2. A similar cluster is found in *A. nidulans* (comparative data analysis at http://www.tigr.org/tigr-scripts/sybil-asp/sybilHome.pl?db=asp). Clustering of genes encoding proteins involved in the same catabolic pathway is not uncommon for filamentous fungi. Enzymatic and regulatory genes for other well-studied catabolic pathways, such as quinate, ethanol, proline, and nitrate utilization, were found to be clustered in various filamentous fungi (reviewed in reference 25). Furthermore, fungal genes involved in secondary metabolism biosynthesis are clustered (5). These clusters also include genes involved in DHN melanin biosynthesis in *A. fumigatus* (30, 52). The existence of the tyrosine degradation cluster in *A. fumigatus* suggests that the genes of this cluster are regulated in a common manner. This is supported by the finding that both genes studied here in more detail, *hmgA* and *hppD*, were shown to be induced at the transcriptional level by L-tyrosine. It is unclear yet how this tyrosine regulation is mediated. Possible regulatory genes, AFUA_2G04210 and AFUA_2G04262, are part of the cluster. It has been shown previously that bacterial homogentisate clusters possess at least one regulatory protein. For example, in *Pseudomonas putida*, the *hmgR* regulatory gene located upstream of *hmgA*, *fahA*, and *maiA* codes for an IclR-type regulator, which acts as a repressor of an aromatic catabolic pathway. It controls the inducible expression of the genes in the homogentisate cluster. HGA is the inducer molecule (1). Further studies will show how the tyrosine signal is transmitted in *A. fumigatus*.

Here, we showed that in *A. fumigatus*, tyrosine degradation is dispensable during growth on minimal agar plates with glucose as the carbon source but essential for growth on agar plates containing L-tyrosine as the sole carbon source. The visible production of pyomelanin requires L-tyrosine or L-phenylalanine in the medium.

It seems likely that L-tyrosine is also present in the lungs of immunosuppressed patients, allowing *A. fumigatus* to produce pyomelanin during infection. Consistently, *A. fumigatus* secretes a variety of proteases (34) during colonization of the lung tissue. It was proposed that protein degradation of the lung tissue is essential for host invasion (27). Indeed, this was proven by the finding that mutants in the methylcitrate synthase of *A. fumigatus* exhibited strongly attenuated virulence due to the accumulation of toxic propionyl-coenzyme A, which derives from the degradation of isoleucine, valine, or methionine. Thus, amino acids are available and serve as nutrient sources during invasive growth (18). This argument is also supported by the finding that L-tyrosine is present in sera at a concentration of between 21 and 107 μM (15) to serve as precursor for a variety of biocompounds, e.g., catecholamines, thyroid hormones, and DOPA melanin. It is also available in tissue due to protein degradation. Furthermore, it can be synthesized from L-phenylalanine by the phenylalanine hydroxylase.

A current model concerning pathogenicity of *A. fumigatus* involving melanin is that conidia are protected from ROI to a certain extent by the DHN melanin pigment and that its biosynthesis genes are also involved in the production of an immunosuppressive compound (4). When conidia germinate and hyphae grow out, e.g., from macrophages, it is conceivable that the formation of pyomelanin further protects the germlings and outgrowing hyphae from ROI, e.g., produced by neutrophils. Consistently, as shown here, by comparing mutant strains with the wild type during growth on agar plates supplemented with L-tyrosine, we found that the Δ*hppD* strain, which lacks pyomelanin, displayed a higher susceptibility to ROI. Similar findings were previously reported for *Burkholderia cenopacia*, and pyomelanin was shown to protect the bacterium from in vitro and in vivo sources of oxidative stress (24). However, the role of ROI in the killing of *A. fumigatus* has been recently challenged since the deletion mutant of the main regulator for the ROI response of *A. fumigatus*, AfYap1, did not influence the killing of *A. fumigatus* by immune effector cells (33). Additionally, as shown here, the Δ*hmgA* deletion mutant characterized by enhanced pyomelanin formation did not show reduced sensitivity to ROI. Therefore, the role of pyomelanin in the scavenging of ROI in vivo remains to be elucidated. Further experiments will show whether the ability to produce pyomelanin influences the pathogenic potential of *A. fumigatus*.

ACKNOWLEDGMENTS

Kim Langfelder and Burghard Liebmann are gratefully acknowledged for initial experiments. We thank Nancy Hannwacker, Silke Steinbach, Ingrid Richter, and Sophia Keller for their excellent technical assistance. We are particularly indebted to Olaf Scheibner for the identification of proteins by mass spectrometry.

This research was supported by the Deutsche Forschungsgemeinschaft (SPP 1160) and the Hans-Knöll-Institute.

REFERENCES

1. **Arias-Barrau, E., E. R. Olivera, J. M. Luengo, C. Fernández, B. Galán, J. L. Garcia, E. Diaz, and B. Miñambres.** 2004. The homogentisate pathway: a central catabolic pathway involved in the degradation of L-phenylalanine, L-tyrosine, and 3-hydroxyphenylacetate in *Pseudomonas putida*. J. Bacteriol. **186:**5062–5077.
2. **Askew, D. S.** 2008. *Aspergillus fumigatus*: virulence genes in a street-smart mold. Curr. Opin. Microbiol. **11:**331–337.
3. **Bilinska, B.** 1996. Progress of infrared investigations of melanin structures. Spectrochim. Acta A **52:**1157–1162.
4. **Brakhage, A. A.** 2005. Systemic fungal infections caused by *Aspergillus* species: epidemiology, infection process and virulence determinants. Curr. Drug Targets **6:**875–886.
5. **Brakhage, A. A., J. Schuemann, S. Bergmann, K. Scherlach, V. Schroeckh, and C. Hertweck.** 2008. Activation of fungal silent gene clusters: a new avenue to drug discovery. Prog. Drug Res. **66:**3–12.
6. **Carreira, A., L. M. Ferreira, and V. Loureiro.** 2001. Brown pigments produced by *Yarrowia lipolytica* result from extracellular accumulation of homogentisic acid. Appl. Environ. Microbiol. **67:**3463–3468.
7. **Coon, S. L., S. Kotob, B. B. Jarvis, S. Wang, W. C. Fuqua, and R. M. Weiner.** 1994. Homogentisic acid is the product of MelA, which mediates melanogenesis in the marine bacterium *Shewanella colwelliana* D. Appl. Environ. Microbiol. **60:**3006–3010.
8. **da Silva Ferreira, M. E., M. R. V. Z. Kress, M. Savoldi, M. H. S. Goldman, A. Härtl, T. Heinekamp, A. A. Brakhage, and G. H. Goldman.** 2006. The *akuB*^{KU80} mutant deficient for nonhomologous end joining is a powerful tool for analyzing pathogenicity in *Aspergillus fumigatus*. Eukaryot. Cell **5:**207–211.
9. **Ellis, M. K., A. C. Whitfield, L. A. Gowans, T. R. Auton, W. M. Provan, E. A. Lock, and L. L. Smith.** 1995. Inhibition of 4-hydroxyphenylpyruvate dioxygenase by 2-(2-nitro-4-trifluoromethylbenzoyl)-cyclohexane-1,3-dione and 2-(2-chloro-4-methanesulfonylbenzoyl)-cyclohexane-1,3-dione. Toxicol. Appl. Pharmacol. **133:**12–19.
10. **Fernández-Cañón, J. M., and M. A. Peñalva.** 1998. Characterization of a fungal maleylacetoacetate isomerase gene and identification of its human homologue. J. Biol. Chem. **273:**329–337.
11. **Fernández-Cañón, J. M., and M. A. Peñalva.** 1995. Fungal metabolic model for human type I hereditary tyrosinaemia. Proc. Natl. Acad. Sci. USA **92:**9132–9136.
12. **Fernández-Cañón, J. M., and M. A. Peñalva.** 1997. Spectrophotometric determination of homogentisate using *Aspergillus nidulans* homogentisate dioxygenase. Anal. Biochem. **245:**218–221.
13. **García-Rivera, J., and A. Casadevall.** 2001. Melanization of *Cryptococcus neoformans* reduces its susceptibility to the antimicrobial effects of silver nitrate. Med. Mycol. **39:**353–357.
14. **Gómez, B. L., and J. D. Nosanchuk.** 2003. Melanin and fungi. Curr. Opin. Infect. Dis. **16:**91–96.
15. **Gressner, A.** 2007. Lexikon der medizinischen Laboratoriumsdiagnostik. Springer, Heidelberg, Germany .
16. **Grosse, C., T. Heinekamp, O. Kniemeyer, A. Gehrke, and A. A. Brakhage.** 2008. Protein kinase A regulates growth, sporulation, and pigment formation in *Aspergillus fumigatus*. Appl. Environ. Microbiol. **74:**4923–4933.
17. **Hamilton, A. J., and B. L. Gómez.** 2002. Melanins in fungal pathogens. J. Med. Microbiol. **51:**189–191.
18. **Ibrahim-Granet, O., M. Dubourdeau, J. P. Latgé, P. Ave, M. Huerre, A. A. Brakhage, and M. Brock.** 2008. Methylcitrate synthase from *Aspergillus fumigatus* is essential for manifestation of invasive aspergillosis. Cell. Microbiol. **10:**134–148.
19. **Jacobson, E. S.** 2000. Pathogenic roles for fungal melanins. Clin. Microbiol. Rev. **13:**708–717.
20. **Jacobson, E. S., and S. B. Tinnell.** 1993. Antioxidant function of fungal melanin. J. Bacteriol. **175:**7102–7104.
21. **Jahn, B., F. Boukhallouk, J. Lotz, K. Langfelder, G. Wanner, and A. A. Brakhage.** 2000. Interaction of human phagocytes with pigmentless *Aspergillus* conidia. Infect. Immun. **68:**3736–3739.
22. **Jahn, B., A. Koch, A. Schmidt, G. Wanner, H. Gehringer, S. Bhakdi, and A. A. Brakhage.** 1997. Isolation and characterization of a pigmentless-conidium mutant of *Aspergillus fumigatus* with altered conidial surface and reduced virulence. Infect. Immun. **65:**5110–5117.
23. **Jahn, B., K. Langfelder, U. Schneider, C. Schindel, and A. A. Brakhage.** 2002. PKSP-dependent reduction of phagolysosome fusion and intracellular kill of *Aspergillus fumigatus* conidia by human monocyte-derived macrophages. Cell. Microbiol. **4:**793–803.
24. **Keith, K. E., L. Killip, P. He, G. R. Moran, and M. A. Valvano.** 2007. *Burkholderia cenocepacia* C5424 produces a pigment with antioxidant properties using a homogentisate intermediate. J. Bacteriol. **189:**9057–9065.
25. **Keller, N. P., and T. M. Hohn.** 1997. Metabolic pathway gene clusters in filamentous fungi. Fungal Genet. Biol. **21:**17–29.
26. **Kniemeyer, O., F. Lessing, O. Scheibner, C. Hertweck, and A. A. Brakhage.** 2006. Optimisation of a 2-D gel electrophoresis protocol for the human-pathogenic fungus *Aspergillus fumigatus*. Curr. Genet. **49:**178–189.
27. **Kogan, T. V., J. Jadoun, L. Mittelman, K. Hirschberg, and N. Osherov.** 2004. Involvement of secreted *Aspergillus fumigatus* proteases in disruption of the actin fiber cytoskeleton and loss of focal adhesion sites in infected A549 lung pneumocytes. J. Infect. Dis. **189:**1965–1973.
28. **Kotob, S. I., S. L. Coon, E. J. Quintero, and R. M. Weiner.** 1995. Homogentisic acid is the primary precursor of melanin synthesis in *Vibrio cholerae*, a *Hyphomonas* strain, and *Shewanella colwelliana*. Appl. Environ. Microbiol. **61:**1620–1622.
29. **Kubodera, T., N. Yamashita, and A. Nishimura.** 2002. Transformation of *Aspergillus* sp. and *Trichoderma reesei* using the pyrithiamine resistance gene (*ptrA*) of *Aspergillus oryzae*. Biosci. Biotechnol. Biochem. **66:**404–406.
30. **Langfelder, K., B. Jahn, H. Gehringer, A. Schmidt, G. Wanner, and A. A. Brakhage.** 1998. Identification of a polyketide synthase gene (*pksP*) of *Aspergillus fumigatus* involved in conidial pigment biosynthesis and virulence. Med. Microbiol. Immunol. **187:**79–89.
31. **Langfelder, K., B. Philippe, B. Jahn, J. P. Latgé, and A. A. Brakhage.** 2001. Differential expression of the *Aspergillus fumigatus pksP* gene detected in vitro and in vivo with green fluorescent protein. Infect. Immun. **69:**6411–6418.
32. **Langfelder, K., M. Streibel, B. Jahn, G. Haase, and A. A. Brakhage.** 2003. Biosynthesis of fungal melanins and their importance for human pathogenic fungi. Fungal Genet. Biol. **38:**143–158.
33. **Lessing, F., O. Kniemeyer, I. Wozniok, J. Loeffler, O. Kurzai, A. Haertl, and A. A. Brakhage.** 2007. The *Aspergillus fumigatus* transcriptional regulator AfYap1 represents the major regulator for defense against reactive oxygen intermediates but is dispensable for pathogenicity in an intranasal mouse infection model. Eukaryot. Cell **6:**2290–2302.
34. **Monod, M., S. Capoccia, B. Léchenne, C. Zaugg, M. Holdom, and O. Jousson.** 2002. Secreted proteases from pathogenic fungi. Int. J. Med. Microbiol. **292:**405–419.
35. **Moran, G. R.** 2005. 4-Hydroxyphenylpyruvate dioxygenase. Arch. Biochem. Biophys. **433:**117–128.
36. **Neuhoff, V., N. Arold, D. Taube, and W. Ehrhardt.** 1988. Improved staining of proteins in polyacrylamide gels including isoelectric focusing gels with clear background at nanogram sensitivity using Coomassie Brilliant Blue G-250 and R-250. Electrophoresis **9:**255–262.

37. **Nosanchuk, J. D., and A. Casadevall.** 2003. The contribution of melanin to microbial pathogenesis. Cell. Microbiol. **5:**203–223.
38. **Nucci, M., and K. A. Marr.** 2005. Emerging fungal diseases. Clin. Infect. Dis. **41:**521–526.
39. **Nunes, L. R., R. Costa de Oliveira, D. B. Leite, V. S. da Silva, E. dos Reis Marques, M. E. da Silva Ferreira, D. C. Ribeiro, L. A. de Souza Bernardes, M. H. Goldman, R. Puccia, L. R. Travassos, W. L. Batista, M. P. Nobrega, F. G. Nóbrega, D. Y. Yang, C. A. de Bragança Pereira, and G. H. Goldman.** 2005. Transcriptome analysis of *Paracoccidioides brasiliensis* cells undergoing mycelium-to-yeast transition. Eukaryot. Cell **4:**2115–2128.
40. **Peñalva, M. A.** 2001. A fungal perspective on human inborn errors of metabolism: alkaptonuria and beyond. Fungal Genet. Biol. **34:**1–10.
41. **Rhodes, J. C., and A. A. Brakhage.** 2006. Molecular determinants of virulence in *Aspergillus fumigatus*, p. 333–345. *In* J. Heitman, S. G. Filler, J. E. Edwards, Jr., and A. P. Mitchell (ed.), Molecular principles of fungal pathogenesis. ASM Press, Washington, DC.
42. **Riley, P. A.** 1997. Melanin. Int. J. Biochem. Cell Biol. **29:**1235–1239.
43. **Rosas, A. L., and A. Casadevall.** 1997. Melanization affects susceptibility of *Cryptococcus neoformans* to heat and cold. FEMS Microbiol. Lett. **153:**265–272.
44. **Ruzafa, C., A. Sanchez-Amat, and F. Solano.** 1995. Characterization of the melanogenic system in *Vibrio cholerae*, ATCC 14035. Pigment Cell Res. **8:**147–152.
45. **Sambrook, J., and D. W. Russell.** 2001. Molecular cloning: a laboratory manual, 3rd ed. Cold Spring Harbor Laboratory Press, Cold Spring Harbor, NY.
46. **Seegmiller, J. E., V. G. Zannoni, L. Laster, and B. N. La Du.** 1961. An enzymatic spectrophotometric method for the determination of homogentisic acid in plasma and urine. J. Biol. Chem. **236:**774–777.
47. **Shevchenko, A., M. Wilm, O. Vorm, and M. Mann.** 1996. Mass spectrometric sequencing of proteins silver-stained polyacrylamide gels. Anal. Chem. **68:**850–858.
48. **Sugareva, V., A. Härtl, M. Brock, K. Hubner, M. Rohde, T. Heinekamp, and A. A. Brakhage.** 2006. Characterisation of the laccase-encoding gene *abr2* of the dihydroxynaphthalene-like melanin gene cluster of *Aspergillus fumigatus*. Arch. Microbiol. **186:**345–355.
49. **Szaniszlo, P. J.** 2002. Molecular genetic studies of the model dematiaceous pathogen *Wangiella dermatitidis*. Int. J. Med. Microbiol. **292:**381–390.
50. **Tekaia, F., and J. P. Latgé.** 2005. *Aspergillus fumigatus*: saprophyte or pathogen? Curr. Opin. Microbiol. **8:**385–392.
51. **Tsai, H.-F., Y. C. Chang, R. G. Washburn, M. H. Wheeler, and K. J. Kwon-Chung.** 1998. The developmentally regulated *alb1* gene of *Aspergillus fumigatus*: its role in modulation of conidial morphology and virulence. J. Bacteriol. **180:**3031–3038.
52. **Tsai, H.-F., M. H. Wheeler, Y. C. Chang, and K. J. Kwon-Chung.** 1999. A developmentally regulated gene cluster involved in conidial pigment biosynthesis in *Aspergillus fumigatus*. J. Bacteriol. **181:**6469–6477.
53. **Wang, Y., and A. Casadevall.** 1994. Decreased susceptibility of melanized *Cryptococcus neoformans* to UV light. Appl. Environ. Microbiol. **60:**3864–3866.
54. **Weidner, G., C. d'Enfert, A. Koch, P. C. Mol, and A. A. Brakhage.** 1998. Development of a homologous transformation system for the human pathogenic fungus *Aspergillus fumigatus* based on the *pyrG* gene encoding orotidine 5′-monophosphate decarboxylase. Curr. Genet. **33:**378–385.
55. **Wheeler, M. H., and A. A. Bell.** 1988. Melanins and their importance in pathogenic fungi. Curr. Top. Med. Mycol. **2:**338–387.
56. **Yabuuchi, E., and A. Ohyama.** 1972. Characterization of "pyomelanin"-producing strains of *Pseudomonas aeruginosa*. Int. J. Syst. Bacteriol. **22:**53–64.